Universal scaling of rotation intervals for quasi-periodically forced circle maps

Glendinning, Paul and Pina-Romero, Silvia

2011

MIMS EPrint: **2011.45**

Manchester Institute for Mathematical Sciences
School of Mathematics

The University of Manchester

Reports available from: http://eprints.maths.manchester.ac.uk/
And by contacting: The MIMS Secretary
School of Mathematics
The University of Manchester
Manchester, M13 9PL, UK

ISSN 1749-9097

Universal scaling of rotation intervals for quasi-periodically forced circle maps

Paul Glendinning

School of Mathematics and
Centre for Interdisciplinary Computational and Dynamical Analysis (CICADA),
University of Manchester, Manchester M13 9PL, U.K.

Silvia Pina-Romero

School of Mathematics, University of Manchester, Manchester M13 9PL, U.K.

Abstract

We introduce a simplifying assumption which makes it possible to approximate the rotation number of an invertible quasi-periodically forced circle map by an integral in the limit of large forcing. We use this to describe universal scaling laws for the width of the non-trivial rotation interval of non-invertible quasi-periodically forced circle maps in this limit, and compare the results with numerical simulations.

Dedicated to the memory of Jaroslav Stark

1. Introduction

Noninvertible circle maps have been used to model the breakdown of invariant tori in differential equations [5, 9], and there are many interesting results about the bifurcation structure for these maps [9, 10]. Whilst invertible maps of the circle have a unique rotation number measuring the average speed of orbits around the circle, noninvertible circle maps have a rotation interval: different orbits can lead to different rotation rates, but the set of all rotation rates is a closed interval, which may be a point [1, 9, 11]. If the differential equation being modelled is quasi-periodically forced then it is

Email address: p.a.glendinning@manchester.ac.uk (Paul Glendinning)

natural to consider an extended system, with an extra variable representing the relative phase of the two frequencies. This leads to systems of the form

$$\begin{aligned} x_{n+1} &= f(x_n, \theta_n) \\ \theta_{n+1} &= \theta_n + \omega, \qquad \omega \in \mathbb{R}\backslash\mathbb{Q} \end{aligned} \tag{1}$$

where $(x, \theta) \in \mathbb{R}^2$, $f(x+1, \theta) = f(x, \theta) + 1$ and $f(x, \theta + 1) = f(x, \theta)$. These conditions imply that it is natural to think of x and θ as taking values modulo one, i.e. representing angles (technically, (1) is the lift of a map of the torus). To fix ideas it is helpful to think of the example,

$$f(x, \theta) = x + a + \frac{b}{2\pi}\sin(2\pi x) + c\sin(2\pi\theta) \tag{2}$$

where a, b and c are real parameters. If $|b| < 1$ then the map is invertible, and this family has been used to consider many aspects of quasi-periodically forced systems including the appearance and bifurcations of strange non-chaotic attractors [2, 3, 4, 7].

If (x_n, θ_n) is the solution of (1) with initial conditions (x_0, θ_0) then classic results due to Herman [8] show that in the invertible case, a well-defined rotation number

$$\rho(x, \theta) = \lim_{n\to\infty} \frac{1}{n}(x_n - x_0) \tag{3}$$

exists and is independent of (x_0, θ_0). In the noninvertible case, Glendinning et al [6] use an argument similar to [1] to show that just as in the unforced circle map the set

$$I = \{r \in \mathbb{R} \mid r = \rho(x, \theta) \text{ some } (x, \theta) \in \mathbb{R}^2\} \tag{4}$$

is a closed interval (possibly trivial) called the rotation interval of the map.

In some sense, the rotation interval gives a measure of the complexity of the system, if it is non-trivial then it implies the existence of uncountably many sets with different rotation rates around the circle. The aim of this note is to prove results about this interval in the limit of large coupling strength (c in the example (2)). Our aim is to derive expressions for the boundary of the rotation interval and hence derive scaling results for the width of the rotation interval as a function of parameters.

2. Quasi-periodically forced maps

To obtain results about the rotation interval in the limit of large coupling strength, we consider smooth maps of the form

$$f(x,\theta) = g(x) + c\Phi(\theta) \tag{5}$$

in the limit of large $|c|$. Here g is the lift of a map of the circle, so $g(x+1) = g(x)+1$ and h is periodic: $\Phi(\theta+1) = \Phi(\theta)$. Moreover, by subtracting off the mean of $c\Phi(\theta)$ and including it in g we may assume that Φ has zero mean:

$$\int_0^1 \Phi(\theta)d\theta = 0. \tag{6}$$

It is often convenient to separate g itself into three parts: first note that the condition $g(x+1) = g(x)+1$ implies that $g(x) = x + \hat{p}(x)$, where $\hat{p}$ has period one. By writing $\hat{p}(x) = a + p(x)$, where a is the mean of $\hat{p}$ we have

$$g(x) = a + x + p(x), \quad p(x+1) = p(x), \quad \int_0^1 p(x)\ dx = 0 \tag{7}$$

where

$$a = \int_0^1 \hat{p}(x)\ dx = \int_0^1 g(x) - x\ dx. \tag{8}$$

Our results are similar in character to those of Ding et al [3]. They consider (1) with f given by (2) in the limit of $0 < b \ll c$ and look to gain insight by neglecting the b term completely and hence studying

$$\begin{array}{ll} x_{n+1} & = x_n + a + c\sin 2\pi\theta_n \\ \theta_{n+1} & = \theta_n + \omega, \quad \omega \in \mathbb{R}\backslash\mathbb{Q} \end{array} \tag{9}$$

Direct calculation shows that $x_n = x_0 + na + c\sum \sin 2\pi\theta_k$, and since $\{\theta_n\}$ is uniformly distributed on the unit circle, the average of $\sin 2\pi\theta_n$ is zero and we obtain the simple expression

$$\rho \sim a$$

which they confirm numerically in the case $c = 6000$, $b = 1$, $0 < a < 0.5$ [3].

Our approach is a little more sophisticated, but yields the same approximation to the rotation number in the invertible case ($|b| < 1$), although we will show that the reason this approximation works so effectively is not

that the b terms in (2) can be ignored at large c, but that solutions for (x_n, θ_n) the set of points (x_n) is approximately uniformly distributed and that $\int_0^1 \sin 2\pi x \; dx = 0$, i.e. the b terms have mean zero.

Figure 1 shows the numerically computed boundary of the rotation interval as a function of a for (2), calculated using an algorithm based on results of [12, 6]. Following Boyland's construction for noninvertible maps of the circle [1], Glendinning et al [6] show that the rotation interval for quasi-periodically forced maps of the form (1), (5) is $I = [\alpha, \beta]$ where α and β are the rotation numbers of the monotonic quasi-periodically forced circle maps with g replaced by G_- and G_+ (respectively) defined by

$$G_-(x) = \inf_{y>x} g(y), \quad G_+(x) = \sup_{y<x} g(y). \tag{10}$$

Stark et al [12] assess numerical methods for computing the rotation number of monotonic quasi-periodically forced circle map, showing that an order $\frac{1}{N}$ bound is possible using an *average* over initial conditions with different initial x_0 of computations using N iterations in (3).

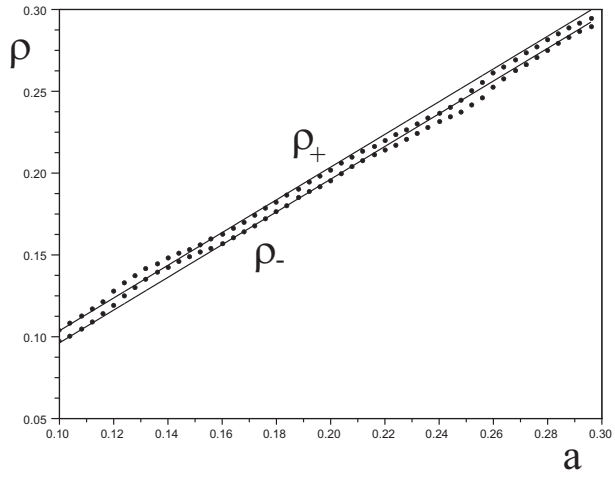

Figure 1: Predicted and approximated borders of the rotation interval for the Arnold map (1) with f given by (2) with parameters $\omega = (\sqrt{5}-1)/2$, $b = 1.18$, $c = 100$ and a varying between 0.1 and 0.3. Rotation numbers on the boundary are calculated using the max/min maps (10) calculated for the Arnold map . Rotation numbers for the max/min maps are calculated by averaging over 8 initial values $(x_0, \theta_0) = (0, k/8)$ with $k = 0, \ldots, 7$ and 50000 iterations were used for each initial condition. The predicted values are represented by the straight lines $\rho = a \pm \frac{9}{8\pi^2}(b-1)^2$, see (35). Note that the predictions are not equally good for all values of a.

3. Scaling results

Figure 1 suggests that as c gets larger, the boundaries of the rotation interval as a function of a become parallel lines. Our first result explains why this is the case, and describes the lines explicitly. Throughout the section we make an assumption about the distribution of points on orbits for which we provide numerical justification in a later section. Our assumption is that *if* $|c|$ *is large then the distribution of points on the orbits of* $G_\pm$ *taken modulo one is nearly uniform in the* $x-$*direction.* We call this the uniform distribution assumption. If we write

$$\rho = \lim_{n\to\infty} \frac{1}{n}(x_n - x_0) \tag{11}$$

where (x_n, θ_n) is the solution of (1) with f given by (5), then by writing g in the form (7) a straightforward calculation yields

$$x_n = na + x_0 + \sum_0^{n-1} p(x_j) + \sum_0^{n-1} \Phi(\theta_j) \tag{12}$$

and hence (11) implies

$$\rho = a + \lim_{n\to\infty} \frac{1}{n} \sum_0^{n-1} p(x_j) + \lim_{n\to\infty} \frac{1}{n} \sum_0^{n-1} \Phi(\theta_j). \tag{13}$$

Since the set (θ_k) is uniformly distributed on $[0, 1)$ as θ evolves under a rigid irrational rotation which preserves Lebesgue (Haar) measure, the second sum tends to zero by (6). Moreover, of the uniform distribution assumption holds then the set (x_k) is approximately uniformly distributed and so

$$\lim_{n\to\infty} \frac{1}{n} \sum_0^{n-1} p(x_j) \approx \int_0^1 p(x)\ dx = 0$$

by (7), where $\approx$ is used to denote equality under the uniform distribution assumption. Hence

$$\rho \approx a = \int_0^1 g(x) - x\ dx. \tag{14}$$

Applying this result ro $G_\pm$ we find $I = [\alpha, \beta]$ where

$$\alpha \approx \int_0^1 (G_-(x) - x)dx, \quad \beta \approx \int_0^1 (G_+(x) - x)dx. \tag{15}$$

Of course, this also allows us to describe the change of I with parameters.

First consider Figure 1 again. This uses the Arnold map (2), and so using (15)

$$\alpha \approx a + K_1, \quad \beta \approx a + K_2 \tag{16}$$

where K_1 and K_2 are integrals which depend only on b (we will find explicit expressions for these integrals in the limit of $b - 1$ small and positive in the next section). Thus the boundaries of the rotation interval in the limit of large c are independent of c to lowest order, and consist of straight lines with unit slope in the (a, ρ) plane.

The integral representation (15) also makes it possible to derive general scaling for the width of the rotation interval in the large coupling limit and near the boundary of invertibility, using (15)

$$|I| = \beta - \alpha \approx \int_0^1 G_+(x) - G_-(x)\ dx. \tag{17}$$

At the boundary of invertibility ($|b| = 1$ for the Arnold map), generically the map g will have a cubic point of inflexion, and local coordinates can be chosen so that $g(x) = A + Cx^3 + O(x^3)$ at this point where $C = \frac{1}{6}g_{xxx}$, with derivatives evaluated at the point of inflexion, which can be assumed to be at the origin. In general we are interested in a family of functions $g(x, \varepsilon)$ with the point of inflexion at $x = 0$ if $\varepsilon = 0$. A small perturbation of this function will be of the form

$$g(x) = A + B\varepsilon_1 x + \varepsilon_2 x^2 + Cx^3$$

to leading order of the parameters, and a shift of the origin can be used to set the x^2 term to zero resulting in the unfolding

$$g(x) = A - \varepsilon Bx + Cx^3 + O(x^4) \tag{18}$$

where

$$B = -g_{x\varepsilon}, \quad C = \tfrac{1}{6}g_{xxx} > 0 \tag{19}$$

(with partial derivatives being evaluated at the point of inflexion with $\varepsilon = 0$). Equation (18) is of course the standard unfolding of a cubic singularity. The small unfolding parameter ε has the property that if $B\varepsilon > 0$ then g is locally invertible, whilst if $B\varepsilon < 0$ then there are two turning points,

$$x_\pm = \pm\sqrt{\frac{B\varepsilon}{3C}} + O(|\varepsilon|^{\frac{3}{2}}) \tag{20}$$

and x_- is the maximum and x_+ is the minimum, and the order of the error term follows by symmetry. Our aim in this section is to prove that *provided the uniform distribution assumption holds* then the length of the rotation interval when $g_{x\varepsilon}\varepsilon < 0$ is, to leading order

$$|I| \sim \frac{9g_{x\varepsilon}^2}{g_{xxx}}\varepsilon^2 \tag{21}$$

For the Arnold map (2) $g(x) = a + x + \frac{b}{2\pi}\sin 2\pi x$ and the point of inflexion is at $x = \frac{1}{2}$ when $b = 1$ and so $\varepsilon = b - 1$, $g_{xb} = -1$, $g_{xxx} = 4\pi^2$ so we predict

$$|I| \sim \frac{9}{2\pi^2}(b-1)^2 \tag{22}$$

which we return to in the next section.

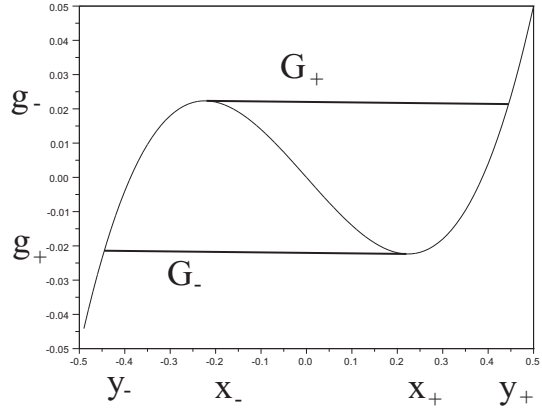

Figure 2: The cubic unfolding showing the upper and lower functions and the geometry of the area representing the rotation interval.

Let $G_\pm$ denote the upper and lower functions (10) for the function defined by (18). Then by symmetry

$$\frac{1}{2}|I| \approx \int_0^{y_+} G_+(x) - G_-(x)\ dx \tag{23}$$

where y_+ is defined by $g(y_+) = g(x_-)$, in other words y_+ is, to lowest order, the new solution of the cubic equation $A - B\varepsilon y + Cy^3 = g(x_-)$ or

$$Cy^3 - B\varepsilon y - \frac{2}{3}B\varepsilon\sqrt{\frac{B\varepsilon}{3C}} = 0.$$

Factorizing this cubic as $(y-x_-)^2(Cy-R)$ and solving for R we obtain

$$y_+ = 2\sqrt{\frac{B\varepsilon}{3C}} + O(|\varepsilon|^{\frac{3}{2}}). \tag{24}$$

The geometry is shown in Figure 2. This shows that we can evaluate the integral (23) in two parts: a rectangle from 0 to x_+ of height $g(x_-)-g(x_+) \sim \frac{4}{3}B\varepsilon\sqrt{\frac{B\varepsilon}{3C}}$ and an integral from x_+ to y_+ with lower boundary f and upper boundary $g(x_-)$, i.e.

$$\frac{1}{2}|I| = \frac{4}{3}B\varepsilon\sqrt{\frac{B\varepsilon}{3C}} \times \sqrt{\frac{B\varepsilon}{3C}} + \int_{x_+}^{y_+} g(x_-) - g(x)\ dx. \tag{25}$$

The remaining integral is elementary:

$$\int_{x_+}^{y_+} g(x_-) - g(x)\ dx = \left[\frac{2}{3}B\varepsilon\sqrt{\frac{B\varepsilon}{3C}}x + \frac{1}{2}B\varepsilon x^2 - \frac{1}{4}Cx^4\right]_{x_+}^{y_+}$$

and direct evaluation gives $\frac{11}{36}\frac{B^2}{C}\varepsilon^2$ and hence

$$\frac{1}{2}|I| \sim \frac{4}{9}B^2\varepsilon^2 C + \frac{11}{36}\frac{B^2\varepsilon^2}{C} = \frac{3}{4}\frac{B^2\varepsilon^2}{C} \tag{26}$$

and hence $|I| \sim \frac{3}{2}\frac{B^2\varepsilon^2}{C}$ which becomes (21) using (19).

To summarize: if the uniform distribution hypothesis is valid (and we give evidence to support its approximate validity at large c) then

- The boundaries of the rotation interval are linear in the mean of the forced circle map, a; and
- Near a cubic singularity with unfolding parameter ε the size of the rotation interval scales like ε^2 in the non-invertible region with a constant of proportionality given explicitly as a ratio of partial derivatives of the map evaluated at the point of inflexion.

4. The Arnold Map

For the special case of the Arnold map (2) the constants K_1 and K_2 of (15) can be calculated explicitly for $b > 1$ with $(b-1)$ small. Moreover, since

(15) is valid even if b is not close to one provided the uniform distribution assumption is still valid, these integrals can be calculated numerically and the results compared with direct numerical computation of the rotation interval's boundaries. At he risk of introducing yet more notation it is convenient to write the Arnold map (2) as

$$g(x) = a + h(x), \quad h(x) = x + \frac{b}{2\pi}\sin(2\pi x) \tag{27}$$

since this means that the constant a can be taken outside the integral in all the evaluations below. We also let $H_\pm$ denote the supremum and infemum functions analogous to (10).

Let

$$b = 1 + \mu^2, \quad \mu > 0. \tag{28}$$

Then the turning points of the Arnold map are at $1 + b\cos(2\pi x) = 0$, $(b > 1)$, and posing an asymptotic expansion of x near $\frac{1}{2}$ in odd powers of μ gives turning points

$$x_\pm \sim \frac{1}{2} \pm \frac{1}{\pi\sqrt{2}}\mu \mp \frac{5}{12\pi\sqrt{2}}\mu^3 + \dots \tag{29}$$

and the local maximum and minimum of $h(x)$ are

$$h_\mp = h(x_\pm) \sim \frac{1}{2} \mp \frac{2}{3\pi\sqrt{2}}\mu^3 + \dots \tag{30}$$

with $h_- < h_+$. Consider the maximum, h_+. We wish to find the $y_+ > \frac{1}{2}$ such that $h(y_+) = h(x_-) = h_+$ (cf. Figure 2). Posing $y_+ \sim \frac{1}{2} + \alpha_1\mu + \alpha_3\mu_+^3 \dots$ and substituting into $h(y_+) = h_+$, with the latter defined by (30) we obtain

$$\frac{2}{3}\pi^2\alpha_1^3 = \alpha_1 - \frac{2}{3\pi\sqrt{2}} = 0 \tag{31}$$

at cubic order, and noting that x_- is a double root of (31) we can factorize to obtain $\alpha_1 = \frac{\sqrt{2}}{\pi}$ and so

$$y_+ \sim \frac{1}{2} + \frac{\sqrt{2}}{\pi}\mu + \dots \tag{32}$$

with $h(y_+) = h_+$. Similarly we find $y_- < \frac{1}{2}$ with $h(y_-) = h_- = h(x_+)$ has

$$y_- \sim \frac{1}{2} - \frac{\sqrt{2}}{\pi}\mu + \dots . \tag{33}$$

Now, the upper boundary of the rotation interval is

$$\rho_+ = \int_0^1 G_+(x) - x \; dx = a + \int_0^1 H_+(x) - x \; dx$$

where G_+ is the supremum function defined via (10), and H_+ the supremum function for h defined in (27). Since H_+ coincides with h except between x_- and y_+ (where, as in the general case $h(y_+) = h_+ = h(x_-)$ with $x_- < \frac{1}{2} < x_+ < y_+$) this integral becomes

$$\rho_+ = a + \int_0^{x_-} \frac{b}{2\pi} \sin 2\pi x \; dx + \int_{x_-}^{y_+} h_+ - x \; dx + \int_{y_+}^1 \frac{b}{2\pi} \sin 2\pi x \; dx$$

and since $\int_0^1 \sin 2\pi x \; dx = 0$ this can be expressed as

$$\rho_+ = a + \int_{x_-}^{y_+} \left(h_+ - (x + \frac{b}{2\pi} \sin 2\pi x) \right) \; dx$$

or

$$\rho_+ \sim a + \left[h_+ x - \frac{1}{2} x^2 + \frac{b}{4\pi^2} \cos 2\pi x \right]_{x_-}^{y_+} \tag{34}$$

Writing $h_+ = \frac{1}{2} + \gamma$, $x_- = \frac{1}{2} - X$ and $y_+ = \frac{1}{2} + Y$, expanding the right hand side of (34) and noting a number of cancelations we find

$$\rho_+ \sim a + \gamma(Y + X) - \frac{1}{2}\mu^2(Y^2 - X^2) - \frac{\pi^2}{6}(Y^4 - X^4).$$

The lowest order terms (which are all that are needed at this stage) are: from (30), $\gamma \sim \frac{2}{3\pi\sqrt{2}}\mu^3$, from (29), $X \sim \frac{1}{\pi\sqrt{2}}\mu$ and from (32), $Y \sim \frac{\sqrt{2}}{\pi}$. Evaluating ρ_+ then gives $\rho_+ \sim a + \frac{9}{8\pi^2}\mu^4$. A precisely similar argument for the lower boundary yields the final result, recalling $\mu^2 = b - 1 > 0$,

$$\rho_\pm \sim a \pm \frac{9}{8\pi^2}(b-1)^2 + O((b-1)^3) \tag{35}$$

from which $|I| = \rho_+ - \rho_- \sim \frac{9}{4\pi^2}(b-1)^2$ follows, cf. (22).

The accuracy of fit of the approximation (35) was shown in Figure 1 earlier with $b = 1.2$. As noted in the figure caption the fit is not uniformly good, and there appears to be an oscillatory modulation (or resonance?) which suggests an interesting correction at next order that we have not investigated. Figure

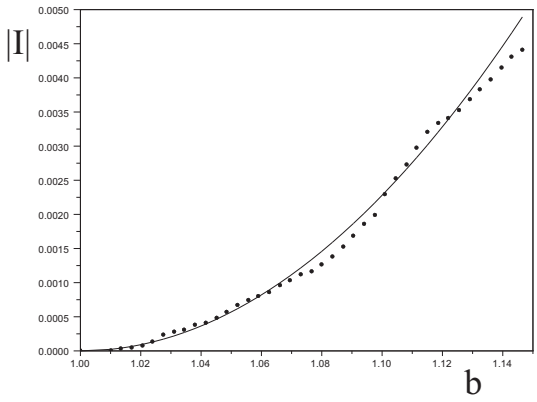

Figure 3: Comparison of numerically computed rotation interval length $|I|$ as a function of b in $b > 1$ (dots) and the theoretical prediction (22). The other parameters are $a = 0.2$, $c = 100$ and $\omega = (\sqrt{5} - 1)/2$.

3 shows the goodness of fit of the quadratic dependence of $|I|$ as a function of b. Again, although the fit is good, there is an obvious oscillation about the theoretical prediction (22).

As noted earlier, the integral representation of the rotation number is a good approximation if the uniform distribution assumption holds. In Figure 4 we show results for larger b, where numerical calculation of the integrals is compared with direct calculation of the rotation interval by computing the rotation numbers using (15). Using the symmetry of the Arnold map, the integral for the theoretical prediction $\rho_\pm \sim a \pm K$ where

$$K = \int_0^1 (H_+(x) - x)dx$$

was computed using a simple trapezoidal rule with 100000 evenly spaced points; for $b = 5$, the case illustrated, this yields $K \approx 0.45435$.

5. Evidence for the uniform distribution assumption

We have not made a detailed analysis of how close the distribution of the points on an orbit must be to uniform in order for our approximations to valid, and it may be possible eventually to put quantitative bounds on the errors due to deviations from the uniform distribution (see the remarks in the conclusion). Here we content ourselves with showing numerically that over many values of c the standard statistical test that would lead one to

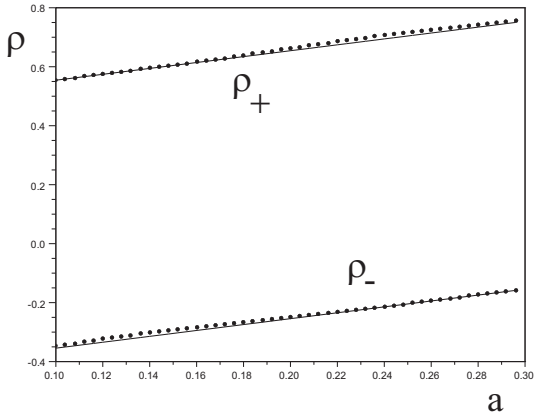

Figure 4: As Figure 1, showing agreement of the theoretical prediction and the rotation numbers computed by iterating the sup and inf maps (10) for the Arnold map (2) with $b = 5$, $c = 100$, $\omega = (\sqrt{5} - 1)/2$.

reject the null hypothesis that the distribution of points is uniform with a confidence of about 1% is *not* satisfied for many values of c.

The Kolmogorov-Smirnov test [13] makes it possible to see how well the distribution of a set of points fits to a null hypothesis that they are drawn from a given probability distribution defined via its cumulative distribution function. In our case the points will be $\{x_0, \ldots, x_{N-1}\}$ obtained by iterating a monotonic quasi-periodically forced circle map with initial conditions (x_0, θ_0), where now we choose to represent the x_i as points in $[0, 1]$ by taking solutions modulo one. Sorting these into increasing order we obtain an increasing sequence $\{y_k\}$ with $0 \leq y_k < y_{k+1} < 1$ which we wish to compare with the cumulative probability distribution of the uniform distribution, which is just the function x. A measure of the deviation from this cumulative distribution function is obtained by looking at

$$D_N = \max\{|y_k - \tfrac{k}{N}|\}$$

and as the sample size tends to infinity $\sqrt{N}D_N$ tends to a known distribution [13]. Note that to be more accurate D_N should be the maximum of $|y_k - \frac{K}{N}|$ and $|y_k - \frac{k-1}{N}|$, but since the difference between the two is of order N^{-2} and we are seeking effects of order $N^{-\frac{1}{2}}$ the definition of D_N above illustrates the point.

The important feature of this is that for a confidence level α we reject the null hypothesis that the sample is uniform if $\sqrt{N}D_N > K_\alpha$, where K_α is

chosen from a distribution satisfying

$$\text{Prob}(K \leq x) = \frac{\sqrt{2\pi}}{x} \sum_{r=0}^{\infty} v^{(2r+1)^2}, \quad v = \exp\left(-\frac{\pi^2}{8x^2}\right)$$

and $\text{Prob}(K \leq K_\alpha) = 1 - \alpha$. Setting $K_\alpha = 5$ numerical calulation based on the first four terms of the sum gives $\text{Prob}(K \leq 5) \approx 0.9894$, corresponding to $\alpha \approx 0.01$.

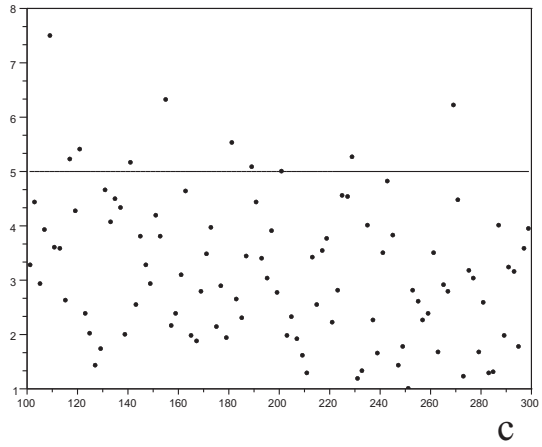

Figure 5: Numerically computed error $\sqrt{N}D_N$ as a function of c for the supremum map of the quasi-periodically forced Arnold map with $a = 0.2$, $b = 1.2$ for a variety of values of c and $N = 100000$. The horizontal line indicates the value $K_\alpha = 5$, and values less than this would not lead to the rejection of the null hypothesis that the points are uniformly distributed with 1% confidence.

Figure 5 shows the results of numerical application of this test for the supremum map of the Arnold map. Note that although there are some cases where $\sqrt{N}D_N$ is greater than 5, and so the null hypothesis would be rejected with $\alpha = 0.01$, it is still relatively small. And the fit is better at larger values of c. Of course, we do not believe that the distribution is actually uniform, so this is perhaps not unsurprising! It could be argued that the independence assumption of the Kolmogorov-Smirnov test is clearly not satisfied by our sequences. However, we have run a similar numerical experiment where every 20^{th} iterate is used (which would allow correlations to decay in a chaotic system) and the results are similar, with slightly fewer points failing the test.

6. Conclusion

We have shown how to calculate approximations to the rotation number of invertible quasi-periodically forced circle maps and the rotation interval in the non-invertible case. We have also demonstrated that the behaviour of the length of this interval just above the point at which the map becomes non-invertible is quadratic with respect to a natural parameter and used the approximations to explore the rotation interval for the quasi-periodically forced circle map.

Our results show good agreement with numerical calculations, but equally that the fit is not uniformly good. There are some parameter values at which the approximations made here are clearly less good than others, and it would be interesting to explore further the dynamical reasons underlying this observation. Since the approximation relies on an approximately uniform distribution of points in the $x-$direction (the fibres of the skew product) the fact that it is less uniform at some parameter values may reflect closeness to resonances.

We also gave a brief numerical justification of the uniform distribution assumption, but did not provide a quantitative estimate of the distance from uniform distribution, nor of the size of the error terms. It may be possible to go some way towards this goal by applying a variant of the Kolmogorov-Smirnov technique which allows one to give the probability that the cumulative distribution function is within some error bound of a given cumulative distribution function – i.e. to write that the cumulative distribution function is within some ϵ of x with a given confidence. Understanding (for example) how this depends on the size of c would help understand the error bounds of the rotation intervals. We have not attempted this more detailed analysis here.

Acknowledgments: PG is partially funded by EPSRC grant EP/E050441/1. SPR is grateful to the University of Manchester and CONACYT.

References

[1] P. Boyland (1986) *Bifurcations of circle maps: Arnold tongues, bistability and rotation intervals*, Commun. Math. Phys. **106** 353-381.

[2] M. Ding, C. Grebogi and E. Ott (1989) *Evolution of attractors in quasiperiodically forced systems: From quasiperiodic to strange nonchaotic to chaotic*, Phys. Rev. A, **39** 2593–2598.

[3] M. Ding, C. Grebogi and E. Ott (1989) *Dimensions of strange non-chaotic attractors* Phys. Lett. A **137** 2593–2598.

[4] U. Feudel, J. Kurths and A. Pikovsky (1995) *Strange non-chaotic attractor in a quasiperiodically forced circle map* Physica D **88** 176–186.

[5] U. Feudel, C. Greborgi and E. Ott (1997) *Phase locking in quasiperiodically forced systems*, Physics Reports **290** 11–25.

[6] P. Glendinning, T. Jäger and J. Stark (2009) *Strangely dispersed minimal sets in the quasiperiodically forced Arnold circle map* Nonlinearity **22** 835-854.

[7] C. Grebogi, E. Ott, S. Pelikan and J.A. Yorke (1984) *Strange attractors that are not chaotic* Physica D **13**, 261–268.

[8] M.R. Herman (1983) *Une méthode pour minorer les exposants de Lyapounov et quelques exemples montrant le caractere local dun théoreme d'Arnold et de Moser sur le tore de dimsnsion 2* Comment. Math. Helv **58** 453–502.

[9] R.S. MacKay and C. Tresser (1986) *Transition to topological chaos for circle maps*, Physica D **19**, 206–237.

[10] R.S. MacKay and C. Tresser (1987) *Some flesh on the skeleton: the bifurcation structure of bimodal maps*, Physica D **27**, 412–422.

[11] M. Misiurewicz (2006) *Rotation theory*, Proceedings of the RIMS Workshop on Dynamical Systems and Applications.

[12] J. Stark, U. Feudel, P. Glendinning and A. Pikovsky (2000) *Rotation numbers for quasiperiodically forced monotone circle maps*, Dyn. Syst. IJ, **17** 1–28.

[13] https://secure.wikimedia.org/wikipedia/en/wiki/Kolmogorov%E2%80%93Smirnov_test (accessed 5 May 2011).